catalysts

MDPI

Article

Gas Phase Catalytic Hydrogenation of C4 Alkynols over Pd/Al_2O_3

Alberto González-Fernández, Chiara Pischetola and Fernando Cárdenas-Lizana *

Chemical Engineering, School of Engineering and Physical Sciences, Heriot Watt University, Edinburgh EH14 4AS, Scotland, UK; ag33@hw.ac.uk (A.G.-F.); cp44@hw.ac.uk (C.P.)

* Correspondence: F.CardenasLizana@hw.ac.uk; Tel.: +44-(0)-131-451-4115

Received: 28 September 2019; Accepted: 1 November 2019; Published: 6 November 2019

Abstract: Alkenols are commercially important chemicals employed in the pharmaceutical and agro-food industries. The conventional production route via liquid phase (batch) alkynol hydrogenation suffers from the requirement for separation/purification unit operations to extract the target product. We have examined, for the first time, the continuous gas phase hydrogenation (P = 1 atm; T = 373 K) of primary (3-butyn-1-ol), secondary (3-butyn-2-ol) and tertiary (2-methyl-3-butyn-2-ol) C_4 alkynols using a 1.2% wt. Pd/Al_2O_3 catalyst. *Post*-TPR, the catalyst exhibited a narrow distribution of $Pd^{\delta-}$ (based on XPS) nanoparticles in the size range 1-6 nm (mean size = 3 nm from STEM). Hydrogenation of the primary and secondary alkynols was observed to occur in a stepwise fashion (-C≡C- → -C=C- → -C-C-) while alkanol formation via direct -C≡C- → -C-C- bond transformation was in evidence in the conversion of 2-methyl-3-butyn-2-ol. Ketone formation via double bond migration was promoted to a greater extent in the transformation of secondary (*vs.* primary) alkynol. Hydrogenation rate increased in the order primary < secondary < tertiary. The selectivity and reactivity trends are accounted for in terms of electronic effects.

Keywords: gas phase hydrogenation; alkynols; 3-butyn-1-ol; 3-butyn-2-ol; 2-methyl-3-butyn-2-ol; alkenols; triple bond electron charge; Pd/Al_2O_3

1. Introduction

The bulk of research on -C≡C- bond hydrogenation has been focused on the transformation of acetylene (to ethylene) over Pd catalysts where the main challenge is to selectively promote semi-hydrogenation with -C=C- formation [1]. Product distribution is influenced by alkyne adsorption/activation mode [2]. Associative adsorption (through a π/σ double bond) on Pd planes [2] follows the Horiuti-Polanyi model, consistent with a stepwise alkyne → alkene → alkane transformation [3,4]. Alternatively, dissociative adsorption via H + three point σ bond [3] or H + π-allyl specie [5] on electron deficient edges/corners of palladium nanoparticles [6] can lead to direct alkyne → alkane hydrogenation [7] or double bond migration [8]. The electronic properties of the palladium phase and the electron density of the -C≡C- bond functionality can influence the alkyne adsorption/activation which, in turn, impact on olefin selectivity. Taking an overview of the published literature, unwanted over-hydrogenation and double migration are prevalent over electron deficient ($Pd^{\delta+}$) nanoparticles that promote strong complexation with the (electron-rich) -C≡C- bond [9,10]. The triple bond charge has also a direct role to play and can be affected by inductive effects (i.e., electron transfer from/to additional groups in poly-functional alkynes). The literature dealing with -C≡C- bond polarisation effects in hydrogenation of multifunctional alkynes is limited. It is, however, worth noting published work that shows increasing activity (over Pd(II) complexes [11] and Pd-Ru catalysts [12]) for hydrogenation of substituted acetylenes with electron donating (e.g., -R=H, $-C_6H_5$, $-CH_3$) functional groups [12]). Terasawa and co-workers [11], investigated the catalytic response for

a series of functionalised alkynes over polymer bounded Pd(II) complexes catalyst and concluded that -C=C- selectivity is sensitive to the nature of the substituent (i.e., increased olefin selectivity in the presence of electron withdrawing substituents (-Cl, -OH) vs. electron donating ($-C_6H_6$) functional groups [12]).

Alkenols have found widespread applications in the manufacture of pharmaceutical (e.g., intermediates for vitamins E, A, K [13] and anti-cancer additives [14]) and agro-food (e.g., dimethyloctenol and citral [13,14]) products. Industrial synthesis involves selective hydrogenation of the correspondent substituted alkynol [15]. Alkynols can be categorised with respect to the number of carbons bonded to the carbon bearing the -OH group (C-α in Figure 1), i.e., primary (one C directly attached; labelled C-β_1), secondary (C-β_1 and C-β_2) and tertiary (C-β_1, C-β_2 and C-β_3).

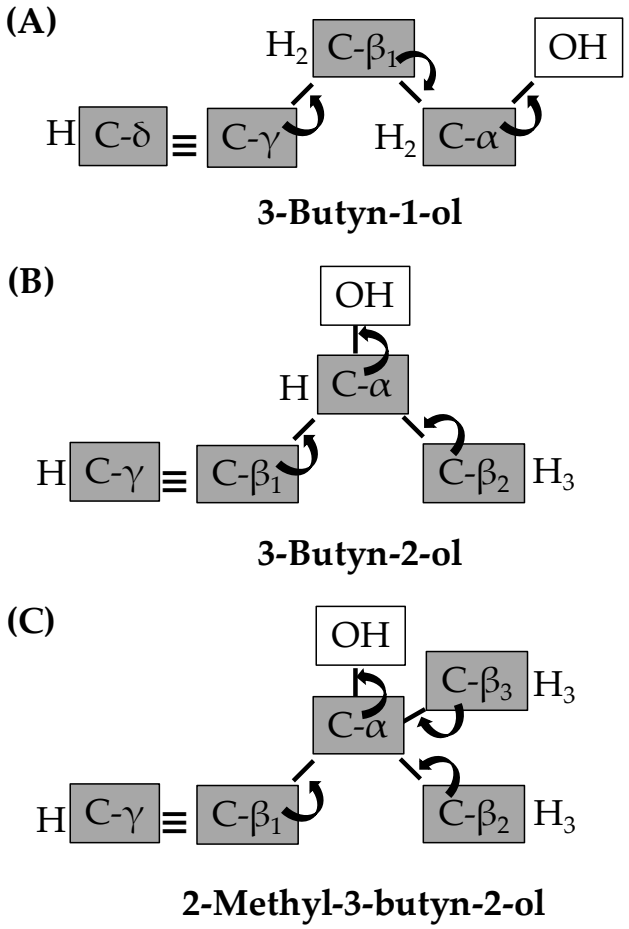

Figure 1. Classification of (**A**) primary, (**B**) secondary and (**C**) tertiary C_4 alkynols. *Note*: Arrows represent associated charge transfer effect.

Work to date has focused on batch liquid mode hydrogenation of saturated (tertiary) alkynols (e.g., 3-methyl-1-pentyn-3-ol [13]) using pressurised (up to 10 atm) reactors [16] with limited research on the selective hydrogenation of primary [17,18] and secondary alkynols [19]. Gas phase continuous operation facilitates control over contact time, which can influence product selectivity [20,21]. We were unable to find any study in the open literature on gas phase hydrogenation of primary or secondary alkynols and only one published paper in the transformation of tertiary alkynols [22]. In this work, we set out to gain an understanding of the mechanism involved in the production of primary alkenols, considering continuous gas phase hydrogenation of 3-butyn-1-ol over a commercial Pd/Al_2O_3 catalyst, as a model system. We extend the catalyst testing to consider secondary and tertiary butynols and prove possible contributions to catalytic performance (i.e., hydrogenation rate and selectivity) due to the position of the hydroxyl group.

2. Results and Discussion

2.1. Catalyst Characterisation

The Pd/Al_2O_3 catalyst used in this study bore, *post*-H_2-temperature programmed reduction (H_2-TPR) to 573 K, metal nanoparticles with diameters ranging from ≤1 nm up to 6 nm (see representative scanning transmission electron microscopy (STEM) image (A) and histogram derived from microscopy analysis (B) in Figure 2) and a number weighted mean diameter of 3 nm. An enhanced intrinsic alkenol selectivity for palladium nanoparticles of 3 nm has been reported elsewhere in the liquid (dehydroisophytol over Pd colloids [23]) and gas phase (2-methyl-3-butyn-2-ol using Pd/SiO_2 [22]) hydrogenation of alkynols. The STEM images reveal a pseudo-spherical morphology, the most thermodynamically stable configuration [6], indicative of a small area of contact at the interface between the Pd nanocrystals and the Al_2O_3 support.

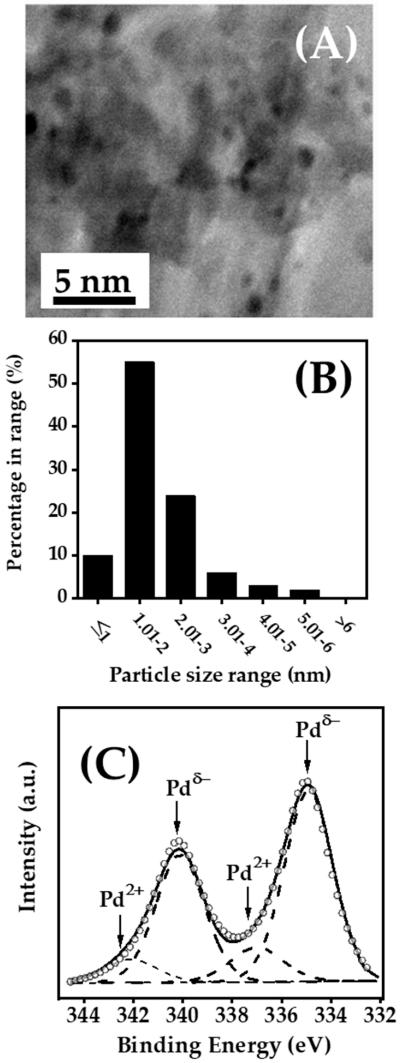

Figure 2. (**A**) Representative scanning transmission electron microscopy (STEM) image with (**B**) associated Pd particle size distribution and (**C**) X-ray photoelectron spectroscopy (XPS) spectrum over the Pd 3*d* region for Pd/Al_2O_3. *Note:* Raw data is shown as symbols (○) while curve fitted (residual standard deviation = 0.14) and envelope is represented by dashed and solid lines, respectively.

X-ray photoelectron spectroscopy (XPS) measurements were carried out to provide insight into the electronic character of the supported Pd phase. The resulting spectra over the Pd 3*d* binding energy (BE) region is shown in Figure 2C. The XPS profile exhibits a doublet with a main Pd $3d_{5/2}$ signal at

334.9 eV, that is 0.3 eV lower than that characteristic of metallic Pd (335.2 eV, [24]), a result that suggests partial electron transfer from OH^- groups on the alumina support [25]. This is consistent with reported (electron-rich) $Pd^{\delta-}$ (4–5 nm) on Al_2O_3 [26]. High (94–97%) butene selectivity has been observed in the hydrogenation of butyne over palladium nanoparticles with a partial negative charge [3]. In contrast, the formation of butane and 2-hexene through undesired over-hydrogenation and double bond migration, respectively, has been reported in the hydrogenation of 1-butyne [8] and 1-hexyne [9] ascribed to the presence of (electron-deficient) $Pd^{\delta+}$ nanocrystals. In addition, the profile shows a weak doublet (12%) with curve-fitted values at higher BE (Pd $3d_{5/2}$ = 337.0 eV; Pd $3d_{3/2}$ = 342.2 eV) that can be ascribed to Pd^{2+} as a result of passivation for ex situ characterisation analyses [27]. A similar (10–12%) percentage value was reported by Weissman et al. [28] attributed to oxygen chemisorption on Pd (111) following a passivation step.

2.2. Reaction Thermodynamics

The calculated change in Gibbs free energy of formation at 373 K for each reaction step ($\Delta G_{(I\text{-}VII)}$) are included in Figure 3.

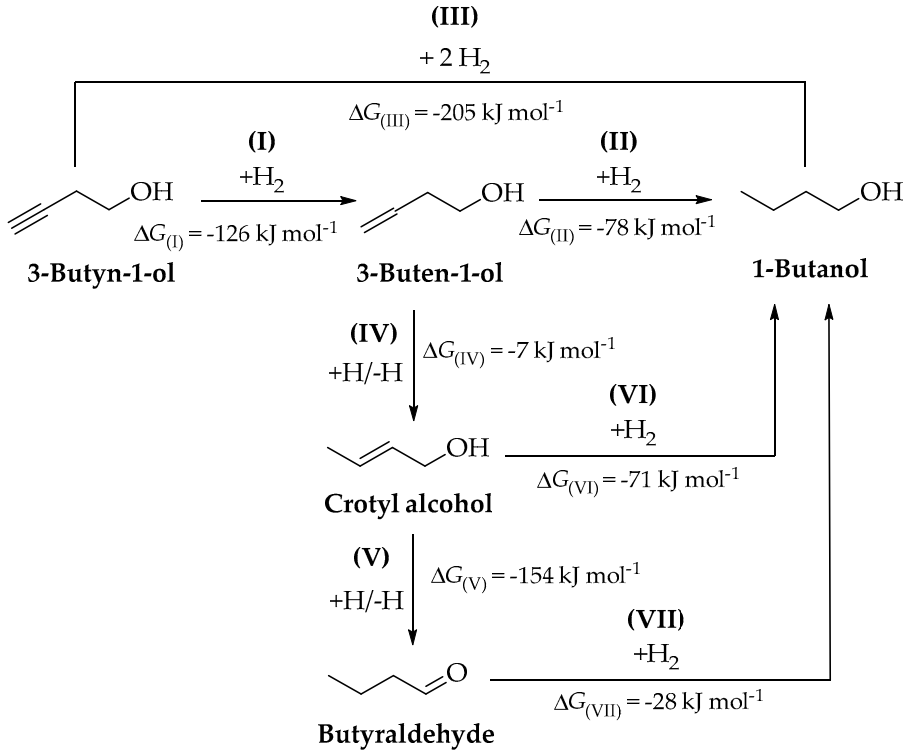

Figure 3. Reaction scheme with Gibbs free energies ($\Delta G_{(I\text{-}VII)}$) for each step in the hydrogenation of primary (3-butyn-1-ol) alkynol: *Reaction conditions*: T = 373 K, P = 1 atm.

The $\Delta G_{(I\text{-}VII)}$ values serve as criteria in the evaluation of thermodynamic feasibility, where reactions can occur spontaneously when $\Delta G < 0$. Each reaction step exhibits negative ΔG indicating that all products considered are thermodynamically favourable. Under our reaction conditions, a thermodynamic analysis of 3-butyn-1-ol hydrogenation established full conversion predominantly to 1-butanol ($S_{1\text{-butanol}}$ > 99%) with trace amounts of butyraldehyde. Formation of alkanol can result from -C=C- reduction in 3-buten-1-ol (step **(II)** in Figure 3) or direct alkynol hydrogenation via step **(III)**. Hydrogenation of the intermediates, that result from alkenol double bond migration (crotyl alcohol (step **(IV)**) and keto-enol tautomerisation (butyraldehyde (step **(V)**), also generates 1-butanol (steps **(VI–VII)**).

2.3. Gas Phase Hydrogenation of 3-Butyn-1-ol

Dependence of hydrogenation path can be effectively proved from a consideration of selectivity as a function of 3-butyn-1-ol conversion; the corresponding data for reaction over Pd/Al_2O_3 is presented in Figure 4.

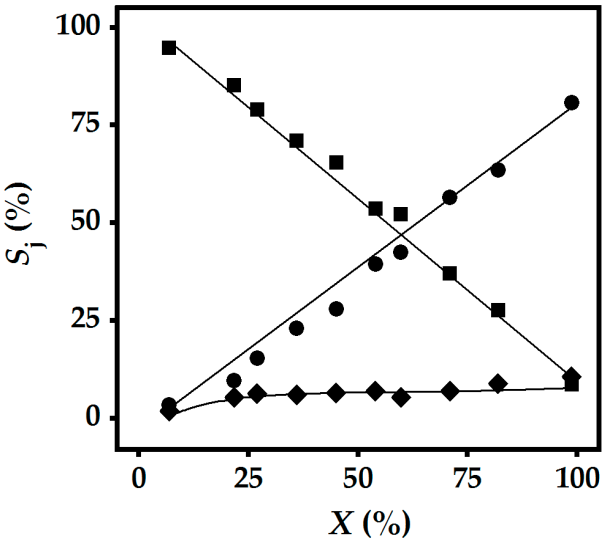

Figure 4. Variation of selectivity (S_j (%), j = 3-buten-1-ol (■), 1-butanol (●), crotyl alcohol+ butyraldehyde (◆) with conversion (X (%)) in hydrogenation of 3-butyn-1-ol over Pd/Al_2O_3. *Note:* solid lines provide a guide to aid visual assessment. *Reaction conditions*: T = 373 K, p = 1 atm.

At low conversions (<25%), product composition deviates from predominant 1-butanol generation under thermodynamic equilibrium, indicative of operation under catalytic control. 3-Buten-1-ol and 1-butanol were the predominant products of partial and full hydrogenation, respectively, but double bond migration (to crotyl alcohol and butyraldehyde) was also detected with a selectivity ≤10%. Formation of 3-buten-1-ol and 1-butanol has been previously reported in the liquid phase (P = 1–6 atm; T = 300–348 K) hydrogenation of 3-butyn-1-ol over MCM-41 [29], Fe_3O_4 [30] and Fe_3O_4 coated SiO_2 [18] supported Pd catalysts. Production of crotyl alcohol and butyraldehyde observed in this work can be linked to reaction temperature (373 K), where T < 353 K serve to avoid double bond migration [31]. A decrease in 3-buten-1-ol selectivity was accompanied by increased formation of 1-butanol at high conversions, indicative of a sequential hydrogenation route (i.e., Horiuti-Polanyi mechanism) from -C≡C- → -C=C- → -C-C-, typical for gas phase alkyne hydrogenations [32].

2.4. Gas Phase Hydrogenation of 3-Butyn-2-ol and 2-Methyl-3-butyn-2-ol

Reaction pathways in the hydrogenation of secondary (3-butyn-2-ol) and tertiary (2-methyl-3-butyn-2-ol) C_4 alkynols are shown in Figure 5.

Both alkynols can undergo sequential (alkynol → alkenol → alkanol, steps **(I-II)**) and direct (alkynol → alkanol, step **(III)**) hydrogenation. Alkenol double bond migration in the transformation of 3-butyn-2-ol generates 2-butanone, (step **(IV)** in Figure 5A) but this step is not possible in the conversion of 2-methyl-3-butyn-2-ol as the C-α (Figure 1) is fully substituted. Alkynol consumption rate at the same degree of conversion (X = 25%) for the three alkynols is presented in Figure 6A where activity decreases in the order: tertiary > secondary > primary. This sequence matches that of decreasing the number of methyl substituents bonded to the C-α (Figure 1), i.e., 2-methyl-3-butyn-2-ol (C-β_1, Cβ_2 and C-β_3) > 3-butyn-2-ol (C-β_1 and C-β_2) > 3-butyn-1-ol (C-β_1). Alkyne hydrogenation has been proposed to proceed via an electrophilic mechanism [12,33]. Reactive hydrogen is provided by dissociative chemisorption of H_2 on Pd [34]. The hydroxyl function can serve to deactivate the triple bond for electrophilic attack through inductive effects by decreasing the overall electron density due to

-C≡C- → -OH electron transfer [35,36]. The presence of (electron donating [37]) methyl substituent(s) bonded to the C-α serves to decrease the "electron-release" from the triple bond (see charge transfer in Figure 1) which favours the electrophilic attack. Our results are in line with the work of Karavanov and Gryaznov [12] who studying the liquid phase hydrogenation of functionalised tertiary alkynols over a Pd-Ru alloy membrane catalyst reported a (40%) enhanced activity as the electron donating character of the substituent increased (i.e., $-CH_2OH < -H < -CH_3$).

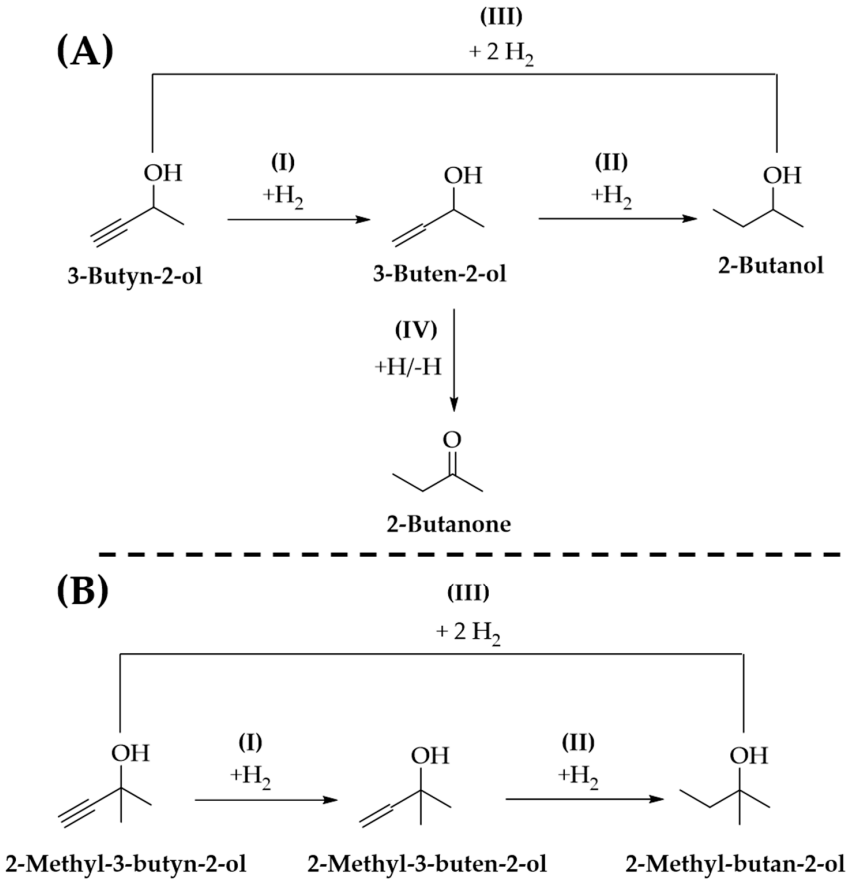

Figure 5. Reaction schemes for the hydrogenation of (**A**) secondary (3-butyn-2-ol) and (**B**) tertiary (2-methyl-3-butyn-2-ol) alkynols.

The results of product selectivity as a function of alkynol conversion for the three C_4 alkynols under consideration are presented in Figure 6B,C. We observe 100% selectivity in terms of -C≡C- → -C=C- bond reduction in the transformation of 3-butyn-1-ol and 3-butyn-2-ol at low conversions where the alkenol selectivity vs. conversion profiles (Figure 6B) for secondary and tertiary alkynols follow a linear decrease of the intermediate concentration as conversion increases, suggesting that they follow the same consecutive hydrogenation route as the primary (steps **(I-II)** in Figures 3 and 5A,B). In each case, regardless of the degree of conversion, greater alkenol selectivity was recorded in the transformation of the primary ~ secondary > tertiary. The lower alkenol selectivity recorded for the tertiary alkynol can be ascribed to direct formation of 2-methyl-butan-2-ol ($S_{\text{2-Methyl-butan-2-ol}}$ = 14% at X ~5%) following step **(III)** in Figure 5B. Semagina et al. [38] using monodispersed Pd nanoparticles in the liquid phase hydrogenation of 2-methyl-3-butyn-2-ol reached a similar conclusion and suggested direct hydrogenation to 2-methyl-butan-2-ol based on the $S_{\text{2-Methyl-3-buten-2-ol}} < 99\%$ at low X. Alkynol dissociative adsorption on (low coordination) Pd sites [39] can lead to direct -C≡C- → -C-C- bond hydrogenation [7] following hydrogen attack of the surface (multi-coordinated) alkilidyne intermediate [3]. This intermediate is generated by H abstraction at the "external" carbon in the -C≡C- bond (e.g., C-δ in 3-butyn-1-ol, Figure 1). Alternatively, double bond migration [8] with

aldehyde/ketone formation (steps **(IV–V)** in Figure 3 and **(IV)** in Figure 5A) can occur as a result of hydrogen addition to the surface π-allyl intermediate generated by hydrogen removal from the carbon bonded to the triple bond functionality (e.g., C-β_1 in 3-butyn-1-ol) [40]. The lower activation energy for the formation of the π-allyl (*vs.* alkylidyne) intermediate [41,42] can account for the absence of direct -C≡C- → -C-C- bond hydrogenation in the conversion of 3-butyn-1-ol and 3-butyn-2-ol. In contrast, hydrogen abstraction in 2-methyl-3-butyn-2-ol is only possible at the (external -C≡C- carbon) C-γ (i.e., no C-α hydrogen) to generate 2-methyl-butan-2-ol. Alkenol double bond migration (*via* hydrogen addition to the external carbon, i.e., C-δ in 3-butyn-1-ol and C-γ in 3-butyn-2-ol, Figure 1, of the π-allyl intermediate [5]) was promoted to a lesser extent in the transformation of 3-butyn-1-ol vs. 3-butyn-2-ol, i.e., higher selectivity to 2-butanone relative to crotyl alcohol + butyraldehyde at all conversions (Figure 6C). Likewise, Bianchini et al. [43] reported a lower isomerisation yield in the liquid phase hydrogenation of 3-buten-1-ol (relative to 3-buten-2-ol) over a Rh complex catalyst. We examined crotyl alcohol and butyraldehyde reactivity in order to assess 1-butanol formation via hydrogenation (steps **(VI)** and **(VII)**, respectively, in Figure 3) and probe selectivity responses. Under similar reaction conditions, we recorded no conversion of butyraldehyde, a response that is consistent with the low capacity of -C=O group (e.g., methyl vinyl ketone and benzalacetone [44]) hydrogenation by Pd [45]. Conversion of crotyl alcohol generated 1-butanol as the sole product but at an appreciable higher (by a factor of 2) rate when compared with that recorded for the 3-butyn-1-ol reaction. The lower double bond migration in terms of crotyl alcohol + butyraldehyde (vs. 2-butanone) generation must result from a more facile transformation of the crotyl alcohol intermediate. Indeed, lack of activity was observed for the conversion of 2-butanone over Pd/Al_2O_3. We acknowledge that catalytic response may not governed by inductive effect alone and the dynamics of surface interactions by the hydrogen reactant can have a major bearing. Future work will be carried out to evaluate the effect of H_2 content in the feed (i.e., Alkynol: H_2 molar ratio) on catalytic performance.

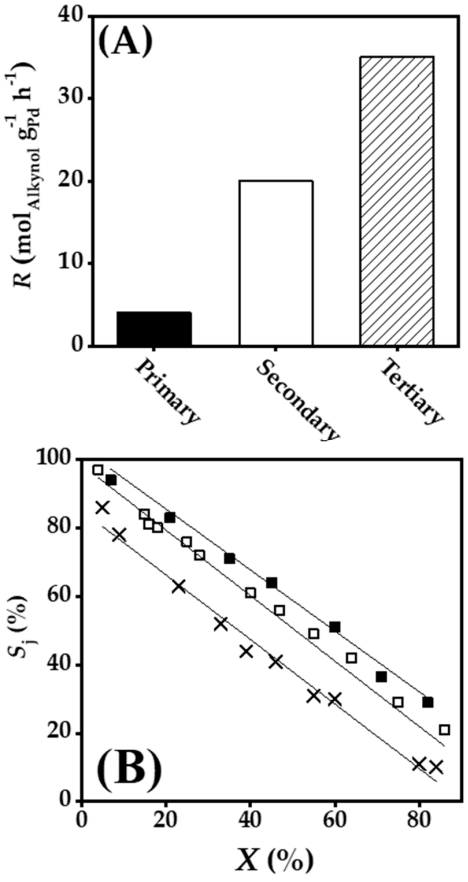

Figure 6. *Cont.*

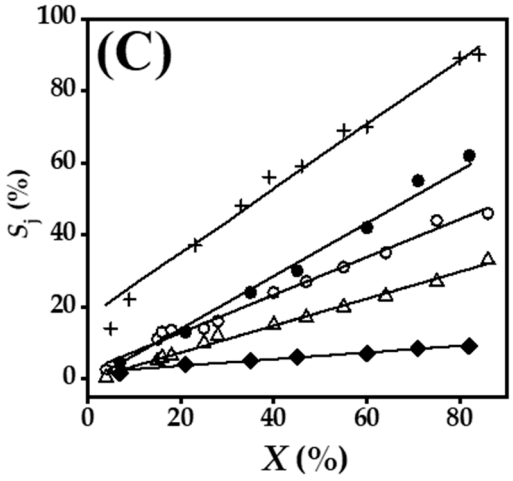

Figure 6. (**A**) Reaction rate (R, $mol_{Alkynol}\ g_{Pd}^{-1}\ h^{-1}$) and variation of selectivity (S_j, %) as a function of conversion (X, %) for products from (**B**) –C≡C– → –C=C– bond partial reduction and (**C**) hydrogen bond migration/reduction in the hydrogenation of primary (solid bar and solid symbols), secondary (open bar and open symbols) and tertiary (hatched bar and crossed symbols) C_4 alkynols over Pd/Al_2O_3; 3-buten-1-ol (■),1-butanol (●), crotyl alcohol + butyraldehyde (◆), 3-buten-2-ol (□), 2-butanol (○), 2-butanone (△), 2-methyl-3-buten-2-ol (×) and 2-methyl-butan-2-ol (+). *Note:* solid lines provide a guide to aid visual assessment. *Reaction conditions*: T = 373 K, p = 1 atm.

3. Materials and Methods

3.1. Catalyst Characterisation

A commercial 1.2% wt. Pd/Al_2O_3 (Sigma-Aldrich, Saint Louis, MO, USA) served as model catalyst. Before use, the catalysts were sieved (ATM fine test sieves) to mean particle diameter = 75 μm and thermally treated in 60 $cm^3\ min^{-1}$ H_2 (BOC, Beijing, China, ≥99.99%) at 2 K min^{-1} to 573 K to ensure reduction to Pd^0 [46]. *Post*-activation, the sample was cooled to ambient temperature and passivated in 1% *v/v* O_2/He (30 $cm^3\ min^{-1}$) for 1 h for ex situ characterisation. Metal particle size and shape was examined by scanning transmission electron microscopy (STEM) using a JEOL 2200FS operated at an accelerating voltage of 200 kV and employing Gatan Digital Micrograph 1.82 for data acquisition/manipulation. The sample was deposited on a holey Cu grid (300 mesh) after dispersion in acetone. The number weighted mean Pd diameter (d) was determined as described elsewhere [47] from a count of 800 particles. X-ray photoelectron spectroscopy (XPS) analyses were conducted on an Axis Ultra instrument (Kratos Analytical, Manchester, UK) under ultra-high vacuum conditions ($<10^{-8}$ Torr) employing a monochromatic Al Kα X-ray source (1486.6 eV). The emitted photoelectrons (source power = 150 W) were sampled from a 750 × 350 μm^2 area at a take-off angle = 90°. The survey (0–1000 eV) and high-resolution spectra (Pd $3d_{5/2}$ and $3d_{3/2}$) were collected with analyser pass energies of 80 and 40 eV, respectively. Charging effects were compensated using the adventitious carbon 1*s* peak calibrated at 284.5 eV as an internal standard. Curve-fitting served to identify/quantify Pd species with modified electronic properties using CasaXPS software in which the Pd 3*d* spectra were fitted with abstraction of the Shirley background using the Gaussian–Lorentzian function with a fixed full width at half maximum (FWHM) of 2.4 and Pd $3d_{5/2}$ intensity of +1.5-fold with respect to Pd $3d_{3/2}$ peak [48]. The goodness of data fitting was based on residual standard deviation; acceptable value ≤ 0.71 [49].

3.2. Catalytic Procedure

All reactions were carried out at T = 373 K at P = 1 atm in situ after activation (in H_2) in a continuous flow fixed bed vertical tubular glass reactor (15 mm i.d.). The operating conditions and catalytic reactor were selected to ensure negligible heat/mass transport limitations. A layer of borosilicate glass beads (1 mm diameter) served as a *pre*-heating zone. A butanolic solution of

the alkynol (3-butyn-1-ol+2-butanol; 3-butyn-2-ol+1-butanol; 2-methyl-3-butyn-2-ol+1-butanol) was vaporised and reached 373 K before contacting the catalyst. In order to maintain isothermal conditions (±1 K) the catalyst bed was diluted with ground glass (75 μm diameter). Reaction temperature was monitored continuously using a thermocouple inserted in a thermowell within the catalyst bed. The reactant was delivered at a fixed calibrated flow rate via a glass/teflon air-tight syringe and Teflon line using a microprocessor-controlled infusion pump (Model 100 kd Scientific). A co-current flow of H_2/N_2 ($P_{H2} \sim 7 \times 10^{-2}$ atm) and alkynol was maintained at $GHSV = 1 \times 10^4$ h^{-1}. The flow rate was continuously monitored with a Humonics (Model 520) digital flowmeter. Molar metal Pd (n) to inlet alkynol molar feed rate (n/F) spanned the range $3 \times 10^{-5} - 368 \times 10^{-4}$ h. In blank tests, reactions in the absence of catalyst or over the Al_2O_3 support alone did not result in any measurable conversion. The reactor effluent was condensed in an ice-bath trap for analysis on a Perkin-Elmer Auto System XL gas chromatograph equipped with a programmed split/splitless injector and a flame ionisation detector using a Stabilwax (fused silica) 30 m × 0.32 mm i.d., 0.25 μm film thickness capillary column (RESTEK, Bellefonte, PA, USA). Data acquisition and manipulation was performed using the TotalChrom Workstation Version 6.1.2 (for Windows) chromatography data system. The solvents (2-butanol (Alpha Aesar, Haverhill, MA, USA, 99%) and 1-butanol (Fisher, The Hamptons, NH, USA, 99.4%)), reactants (3-butyn-1-ol (Aldrich, Beijing, China, 97%), 3-butyn-2-ol (Aldrich, 97%) and 2-methyl-3-butyn-2-ol (Aldrich, 98%)) and products (3-buten-1-ol (Aldrich, 96%), 1-butanol (Aldrich, 99%), crotyl alcohol (Aldrich, 96%), butyraldehyde (Aldrich, 96%), 3-buten-2-ol (Aldrich, 97%), 2-butanol (Aldrich, 99.5%), 2-butanone (Aldrich, 99%), 2-methyl-3-buten-2-ol (Aldrich, 98%), 2-methyl-butan-2-ol (Aldrich, 99%)) were used without further purification. Reactant and product molar fractions (x_i) were obtained using detailed calibration plots (not shown). Catalytic performance is considered in terms of conversion (X) at steady state after 3 h on-stream:

$$X(\%) = \frac{[\text{Alkynol}]_{in} - [\text{Alkynol}]_{out}}{[\text{Alkynol}]_{in}} \times 100 \quad (1)$$

while selectivity to product j (S_j) was obtained from:

$$S_j(\%) = \frac{\left[\text{Product}_j\right]_{out}}{[\text{Alkynol}]_{in} - [\text{Alkynol}]_{out}} \times 100 \quad (2)$$

where the subscripts "in" and "out" represent the inlet and outlet streams. Catalytic activity is also quantified in terms of alkynol consumption rate (R, $mol_{Alkynol}\ g_{Pd}{}^{-1}\ h^{-1}$) according to the procedure described elsewhere [50]. Reactions were repeated with the same batch of catalyst delivering a carbon mass balance and raw data reproducibility within ±6%.

3.3. Thermodynamic Analysis

The thermodynamic analysis of catalytic processes provides critical information in terms of highest conversion/selectivity possible under specific operating conditions. All the reactant and products involved in the hydrogenation of 3-butyn-1-ol (as representative) were considered (3-butyn-1-ol, 3-buten-1-ol, 1-butanol, crotyl alcohol, butyraldehyde and H_2). The inlet 3-butyn-1-ol was set at 1 mol and product distribution determined at equilibrium where T = 373 K, P = 1 atm and H_2: Alkynol molar ratio = 2 to mimic catalytic reaction conditions. Aspen Plus was used to make the equilibrium calculations [51] in order to extract product distribution in a system with minimised Gibbs free energy using the method of group contribution [52].

4. Conclusions

We have examined the effect of -OH group position on catalytic gas phase hydrogenation of C_4 alkynols over Pd/Al_2O_3 ($Pd^{\delta-}$ nanoparticles with mean (number weighted) size = 3 nm). A

correlation between the number of electron-donating (-CH_3) groups and catalytic activity has been established consistent with the following decreasing activity sequence: tertiary (2-methyl-3-butyn-2-ol) > secondary (3-butyn-2-ol) > primary (3-butyn-1-ol). The conversion of primary and secondary alkynols follows a stepwise (alkynol → alkenol → alkanol) reaction mechanism while direct alkynol → alkanol transformation was a feature of 2-methyl-3-butyn-2-ol hydrogenation. Double bond migration is promoted to a greater extent in the transformation of 3-butyn-2-ol relative to 3-butyn-1-ol consistent with crotyl alcohol hydrogenation. The results in this work establish the role of -C≡C- polarity in determining the activity/selectivity pattern for the synthesis of valuable alkenols.

Author Contributions: F.C.-L. conceived the idea and was in charge of overall direction and planning of the project; A.G.-F. carried out the experiments; A.G.-F. and C.P. wrote the manuscript with input from F.C.-L.

Funding: This research was funded by the Engineering and Physical Sciences Research Council EPRSC grant number EP/L016419/1 [studentship to Alberto González-Fernández and Chiara Pischetola, CRITICAT program].

Acknowledgments: Open Access Funding by Heriot-Watt University.

Conflicts of Interest: The authors declare no conflict of interest.

References

1. Delgado, J.A.; Benkirane, O.; Claver, C.; Curulla-Ferré, D.; Godard, C. Advances in the Preparation of Highly Selective Nanocatalysts for the Semi-Hydrogenation of Alkynes Using Colloidal Approaches. *Dalton Trans.* **2017**, *46*, 12381–12403. [CrossRef]
2. Rajaram, J.; Narula, A.P.S.; Chawla, H.P.S.; Dev, S. Semihydrogenation of Acetylenes. *Tetrahedron* **1983**, *39*, 2315–2322. [CrossRef]
3. Molnár, Á.; Sárkány, A.; Varga, M. Hydrogenation of Carbon-Carbon Multiple Bonds: Chemo-, Regio- and Stereo-Selectivity. *J. Mol. Catal. A Chem.* **2001**, *173*, 185–221. [CrossRef]
4. Mei, D.; Sheth, P.; Neurock, M.; Smith, C. First-Principles-Based Kinetic Monte Carlo Simulation of the Selective Hydrogenation of Acetylene over Pd(111). *J. Catal.* **2006**, *242*, 1–15. [CrossRef]
5. Karpiński, Z. Catalysis by Supported, Unsupported, and Electron-Deficient Palladium. In *Advances in Catalysis*; Academic Press: Warsaw, Poland, 1990; Volume 37, pp. 45–100.
6. Semagina, N.; Kiwi-Minsker, L. Recent Advances in the Liquid-Phase Synthesis of Metal Nanostructures with Controlled Shape and Size for Catalysis. *Catal. Rev.* **2009**, *51*, 147–217. [CrossRef]
7. Sárkány, A.; Weiss, A.H.; Guczi, L. Structure Sensitivity of Acetylene-Ethylene Hydrogenation over Pd Catalysts. *J. Catal.* **1986**, *98*, 550–553. [CrossRef]
8. Hub, S.; Touroude, R. Mechanism of Catalytic Hydrogenation of But-1-yne on Palladium. *J. Catal.* **1988**, *114*, 411–421. [CrossRef]
9. Semagina, N.; Renken, A.; Kiwi-Minsker, L. Palladium Nanoparticle Size Effect in 1-Hexyne Selective Hydrogenation. *J. Phys. Chem. C* **2007**, *111*, 13933–13937. [CrossRef]
10. Boitiaux, J.P.; Cosyns, J.; Vasudevan, S. Hydrogenation of Highly Unsaturated Hydrocarbons over Highly Dispersed Pd Catalyst. Part II: Ligand Effect of Piperidine. *Appl. Catal.* **1985**, *15*, 317–326. [CrossRef]
11. Terasawa, M.; Yamamoto, H.; Kaneda, K.; Imanaka, T.; Teranishi, S. Selective Hydrogenation of Acetylenes to Olefins Catalyzed by Polymer-Bound Palladium(II) Complexes. *J. Catal.* **1979**, *57*, 315–325. [CrossRef]
12. Karavanov, A.N.; Gryaznov, V.M. Effect of the Structure of Substituted Propargyl and Allyl Alcohols on the Rate of their Liquid Phase Hydrogenation on a Pd-Ru Alloy Membrane Catalyst. *Bull. Acad. Sci. USSR Division Chem. Sci.* **1989**, *38*, 1593–1596. [CrossRef]
13. Bonrath, W.; Netscher, T. Catalytic Processes in Vitamins Synthesis and Production. *Appl. Catal. A Gen.* **2005**, *280*, 55–73. [CrossRef]
14. Bonrath, W.; Medlock, J.; Schütz, J.; Wüstenberg, B.; Netscher, T. Hydrogenation in the Vitamins and Fine Chemicals Industry—An Overview. In *Hydrogenation*; InTech: Rijeka, Croatia, 2012; pp. 69–90.
15. Bonrath, W.; Eggersdorfer, M.; Netscher, T. Catalysis in the Industrial Preparation of Vitamins and Nutraceuticals. *Catal. Today* **2007**, *121*, 45–57. [CrossRef]
16. Crespo-Quesada, M.; Cárdenas-Lizana, F.; Dessimoz, A.L.; Kiwi-Minsker, L. Modern Trends in Catalyst and Process Design for Alkyne Hydrogenations. *ACS Catal.* **2012**, *2*, 1773–1786. [CrossRef]

17. Izumi, Y.; Tanaka, Y.; Urabe, K. Selective Catalytic Hydrogenation of Propargyl Alcohol with Heteropoly Acid-Modified Palladium. *Chem. Lett.* **1982**, *11*, 679–682. [CrossRef]
18. Uberman, P.M.; Costa, N.J.S.; Philippot, K.; Carmona, R.; dos Santos, A.A.; Rossi, L.M. A Recoverable Pd Nanocatalyst for Selective Semi-Hydrogenation of Alkynes: Hydrogenation of Benzyl-Propargylamines as a Challenging Model. *Green Chem.* **2014**, *16*, 4566–4574. [CrossRef]
19. Navarro-Fuentes, F.; Keane, M.; Ni, X.-W. A Comparative Evaluation of Hydrogenation of 3-Butyn-2-ol over Pd/Al_2O_3 in an Oscillatory Baffled Reactor and a Commercial Parr Reactor. *Org. Process Res. Dev.* **2019**, *23*, 38–44. [CrossRef]
20. Hou, R.; Wang, T.; Lan, X. Enhanced Selectivity in the Hydrogenation of Acetylene due to the Addition of a Liquid Phase as a Selective Solvent. *Ind. Eng. Chem. Res.* **2013**, *52*, 13305–13312. [CrossRef]
21. Pérez, D.; Olivera-Fuentes, C.; Curbelo, S.; Rodríguez, M.J.; Zeppieri, S. Study of the Selective Hydrogenation of 1,3-Butadiene in Three Types of Industrial Reactors. *Fuel* **2015**, *149*, 34–45. [CrossRef]
22. Prestianni, A.; Crespo-Quesada, M.; Cortese, R.; Ferrante, F.; Kiwi-Minsker, L.; Duca, D. Structure Sensitivity of 2-Methyl-3-Butyn-2-ol Hydrogenation on Pd: Computational and Experimental Modeling. *J. Phys. Chem. C* **2014**, *118*, 3119–3128. [CrossRef]
23. Yarulin, A.; Yuranov, I.; Cárdenas-Lizana, F.; Abdulkin, P.; Kiwi-Minsker, L. Size-Effect of Pd-(Poly(*N*-vinyl-2-pyrrolidone)) Nanocatalysts on Selective Hydrogenation of Alkynols with Different Alkyl Chains. *J. Phys. Chem. C* **2013**, *117*, 13424–13434. [CrossRef]
24. Smirnov, M.Y.; Klembovskii, I.O.; Kalinkin, A.V.; Bukhtiyarov, V.I. An XPS Study of the Interaction of a Palladium Foil with NO_2. *Kinet. Catal.* **2018**, *59*, 786–791. [CrossRef]
25. Juan-Juan, J.; Román-Martínez, M.C.; Illán-Gómez, M.J. Catalytic Activity and Characterization of Ni/Al_2O_3 and NiK/Al_2O_3 Catalysts for CO_2 Methane Reforming. *Appl. Catal. A Gen.* **2004**, *264*, 169–174. [CrossRef]
26. Nag, N.K. A Study on the Dispersion and Catalytic Activity of Gamma Alumina-Supported Palladium Catalysts. *Catal. Lett.* **1994**, *24*, 37–46. [CrossRef]
27. McCarty, J.G. Kinetics of PdO Combustion Catalysis. *Catal. Today* **1995**, *26*, 283–293. [CrossRef]
28. Weissman, D.L.; Shek, M.L.; Spicer, W.E. Photoemission Spectra and Thermal Desorption Characteristics of Two States of Oxygen on Pd. *Surf. Sci.* **1980**, *92*, L59–L66. [CrossRef]
29. Papp, A.; Molnár, Á.; Mastalir, Á. Catalytic Investigation of Pd Particles Supported on MCM-41 for the Selective Hydrogenations of Terminal and Internal Alkynes. *Appl. Catal. A Gen.* **2005**, *289*, 256–266. [CrossRef]
30. Da Silva, F.P.; Rossi, L.M. Palladium on Magnetite: Magnetically Recoverable Catalyst for Selective Hydrogenation of Acetylenic to Olefinic Compounds. *Tetrahedron* **2014**, *70*, 3314–3318. [CrossRef]
31. Derrien, M.L. Selective Hydrogenation Applied to the Refining of Petrochemical Raw Materials Produced by Steams Cracking. *Stud. Surf. Sci. Catal.* **1986**, *27*, 613–666.
32. Nikolaev, S.A.; Zanaveskin, L.N.; Smirnov, V.V.; Averyanov, V.A.; Zanaveskin, K.L. Catalytic Hydrogenation of Alkyne and Alkadiene Impurities from Alkenes. Practical and Theoretical Aspects. *Russ. Chem. Rev.* **2009**, *78*, 231–247. [CrossRef]
33. Morrill, C.; Grubbs, R.H. Highly Selective 1,3-Isomerization of Allylic Alcohols via Rhenium Oxo Catalysis. *J. Am. Chem. Soc.* **2005**, *127*, 2842–2843. [CrossRef]
34. Jewell, L.; Davis, B. Review of Absorption and Adsorption in the Hydrogen–Palladium System. *Appl. Catal. A Gen.* **2006**, *310*, 1–15. [CrossRef]
35. Nikoshvili, L.; Shimanskaya, E.; Bykov, A.; Yuranov, I.; Kiwi-Minsker, L.; Sulman, E. Selective Hydrogenation of 2-Methyl-3-Butyn-2-ol over Pd-Nanoparticles Stabilized in Hypercrosslinked Polystyrene: Solvent Effect. *Catal. Today* **2014**, *241*, 179–188. [CrossRef]
36. Sulman, E.M. Selective Hydrogenation of Unsaturated Ketones and Acetylene Alcohols. *Russ. Chem. Rev.* **1994**, *63*, 923–936. [CrossRef]
37. Hansch, C.; Leo, A.; Taft, R.W. A Survey of Hammett Substituent Constants and Resonance and Field Parameters. *Chem. Rev.* **1991**, *91*, 165–195. [CrossRef]
38. Semagina, N.; Renken, A.; Laub, D.; Kiwi-Minsker, L. Synthesis of Monodispersed Palladium Nanoparticles to Study Structure Sensitivity of Solvent-Free Selective Hydrogenation of 2-Methyl-3-butyn-2-ol. *J. Catal.* **2007**, *246*, 308–314. [CrossRef]

39. Boitiaux, J.P.; Cosyns, J.; Robert, E. Liquid Phase Hydrogenation of Unsaturated Hydrocarbons on Palladium, Platinum and Rhodium Catalysts. Part II: Kinetic Study of 1-Butene, 1,3-Butadiene and 1-Butyne Hydrogenation on Rhodium; Comparison with Platinum and Palladium Part II. *Appl. Catal.* **1987**, *32*, 169–183. [CrossRef]
40. Morrill, T.C.; D'Souza, C.A. Efficient Hydride-Assisted Isomerization of Alkenes via Rhodium Catalysis. *Organometallics* **2003**, *22*, 1626–1629. [CrossRef]
41. Karlsson, E.A.; Bäckvall, J.-E. Mechanism of the Palladium-Catalyzed Carbohydroxylation of Allene-Substituted Conjugated Dienes: Rationalization of the Recently Observed Nucleophilic Attack by Water on a (π-Allyl)palladium Intermediate. *Chem. A Eur. J.* **2008**, *14*, 9175–9180. [CrossRef]
42. Behm, R.J.; Penka, V.; Cattania, M.-G.; Christmann, K.; Ertl, G. Evidence for '"Subsurface"' Hydrogen on Pd(110): An Intermediate Between Chemisorbed and Dissolved Species. *J. Chem. Phys.* **1983**, *78*, 7486–7490. [CrossRef]
43. Bianchini, C.; Meli, A.; Oberhauser, W. Isomerization of Allylic Alcohols to Carbonyl Compounds by Aqueous-Biphase Rhodium Catalysis. *New J. Chem.* **2001**, *25*, 11–12. [CrossRef]
44. Ide, M.S.; Hao, B.; Neurock, M.; Davis, R.J. Mechanistic Insights on the Hydrogenation of α,β-Unsaturated Ketones and Aldehydes to Unsaturated Alcohols over Metal Catalysts. *ACS Catal.* **2012**, *2*, 671–683. [CrossRef]
45. Ponec, V. On the Role of Promoters in Hydrogenations on Metals; α,β-Unsaturated Aldehydes and Ketones. *Appl. Catal. A Gen.* **1997**, *149*, 27–48. [CrossRef]
46. Amorim, C.; Keane, M.A. Palladium Supported on Structured and Nonstructured Carbon: A Consideration of Pd Particle Size and the Nature of Reactive Hydrogen. *J. Colloid Interface Sci.* **2008**, *322*, 196–208. [CrossRef] [PubMed]
47. Cárdenas-Lizana, F.; Wang, X.; Lamey, D.; Li, M.; Keane, M.A.; Kiwi-Minsker, L. An Examination of Catalyst Deactivation in *p*-Chloronitrobenzene Hydrogenation over Supported Gold. *Chem. Eng. J.* **2014**, *255*, 695–704. [CrossRef]
48. Venezia, A.M.; Liotta, L.F.; Deganello, G.; Schay, Z.; Guczi, L. Characterization of Pumice-Supported Ag–Pd and Cu–Pd Bimetallic Catalysts by X-Ray Photoelectron Spectroscopy and X-Ray Diffraction. *J. Catal.* **1999**, *182*, 449–455. [CrossRef]
49. Fu, Z.; Hu, J.; Hu, W.; Yang, S.; Luo, Y. Quantitative analysis of Ni^{2+}/Ni^{3+} in $Li[Ni_xMn_yCo_z]O_2$ Cathode Materials: Non-linear Least-squares Fitting of XPS Spectra. *Appl. Surf. Sci.* **2018**, *441*, 1048–1056. [CrossRef]
50. Cárdenas-Lizana, F.; Lamey, D.; Perret, N.; Gómez-Quero, S.; Kiwi-Minsker, L.; Keane, M.A. Au/Mo_2N as a New Catalyst Formulation for the Hydrogenation of *p*-Chloronitrobenzene in Both Liquid and Gas Phases. *Catal. Commun.* **2012**, *21*, 46–51. [CrossRef]
51. Ye, G.; Xie, D.; Qiao, W.; Grace, J.R.; Lim, C.J. Modelling of Fluidized Bed Membrane Reactors for Hydrogen Production from Steam Methane Reforming with Aspen Plus. *Int. J. Hydrogen Energy* **2009**, *34*, 4755–4762. [CrossRef]
52. Joback, K.G.; Reid, R.C. Estimation of Pure-Component Properties from Group-Contributions. *Chem. Eng. Commun.* **1987**, *57*, 233–243. [CrossRef]